nature water

Article

https://doi.org/10.1038/s44221-023-00077-6

Substantial defluorination of polychlorofluorocarboxylic acids triggered by anaerobic microbial hydrolytic dechlorination

Received: 29 June 2022

Accepted: 4 April 2023

Published online: 15 May 2023

Check for updates

Bosen Jin[1], Huaqing Liu[1], Shun Che[1,2], Jinyu Gao[1], Yaochun Yu[1,2], Jinyong Liu[1] & Yujie Men[1,2]

Chlorinated polyfluorocarboxylic acids (Cl-PFCAs) derived from the widely used chlorotrifluoroethylene oligomers and polymers may enter and influence the aquatic environment. Here we report the substantial defluorination of Cl-PFCAs by an anaerobic microbial community via novel pathways triggered by anaerobic microbial dechlorination. Cl-PFCAs first underwent microbial reductive, hydrolytic and eliminative dechlorination, with the hydrolytic dechlorination leading to the highest spontaneous defluorination. Hydrolytic dechlorination was favoured with increased Cl substitutions. An isolated, highly enriched, anaerobic defluorinating culture was dominated by two genomes that were most similar to those of *Desulfovibrio aminophilus* and *Sporomusa sphaeroides*, both of which exhibited defluorination activity towards chlorotrifluoroethylene tetramer acid. The results imply that anaerobic non-respiratory hydrolytic dechlorination plays a critical role in the fate of chlorinated polyfluoro chemicals in natural and engineered water environments. The greatly enhanced biodegradability by Cl substitution also sheds light on the design of cost-effective treatment biotechnologies, as well as alternative polyfluoroalkyl substances that are readily biodegradable and less toxic.

Polychlorofluoroalkyl compounds represent a large group of per- and polyfluoroalkyl substances (PFAS), which have found widespread use in commercial products and industrial materials[1–5]. Well-known examples include fluoropolymers such as polychlorotrifluoroethylene (PCTFE)[3,6] and chlorotrifluoroethylene (CTFE) oligomers contained in non-flammable hydraulic fluid[7,8]. The thermolysis of PCTFE and metabolism of CTFE oligomers by higher organisms can generate CTFE oligomer carboxylic acids[9–13]. They may enter into the hydrosphere together with other chlorinated PFAS (Cl-PFAS)[14] and ultra-short-chain chlorofluorocarboxylic acids used as building blocks for PFAS synthesis[15] or derived from chlorofluorocarbons[16,17], causing adverse impacts on the ecosystem. Compared with strong C–F bonds, which have shown sluggish microbial cleavage in a limited number of PFAS structures[18–21], C–Cl bonds have a lower bond dissociation energy (BDE) and are more readily cleaved microbially[22]. Thus, the C–Cl bonds in Cl-PFAS could be vulnerable positions for microbial attack, thereby enhancing their biodegradability and even defluorination activity.

Despite the increasing detection of Cl-PFAS in diverse natural and engineered environments, including surface run-off, lakes, sediments and WWTPs[23–28], their biodegradability and environmental fate are

[1]Department of Chemical and Environmental Engineering, University of California, Riverside, Riverside, CA, USA. [2]Department of Civil and Environmental Engineering, University of Illinois at Urbana-Champaign, Urbana, IL, USA. e-mail: ymen@engr.ucr.edu

https://doi.org/10.1038/s44221-023-00077-6

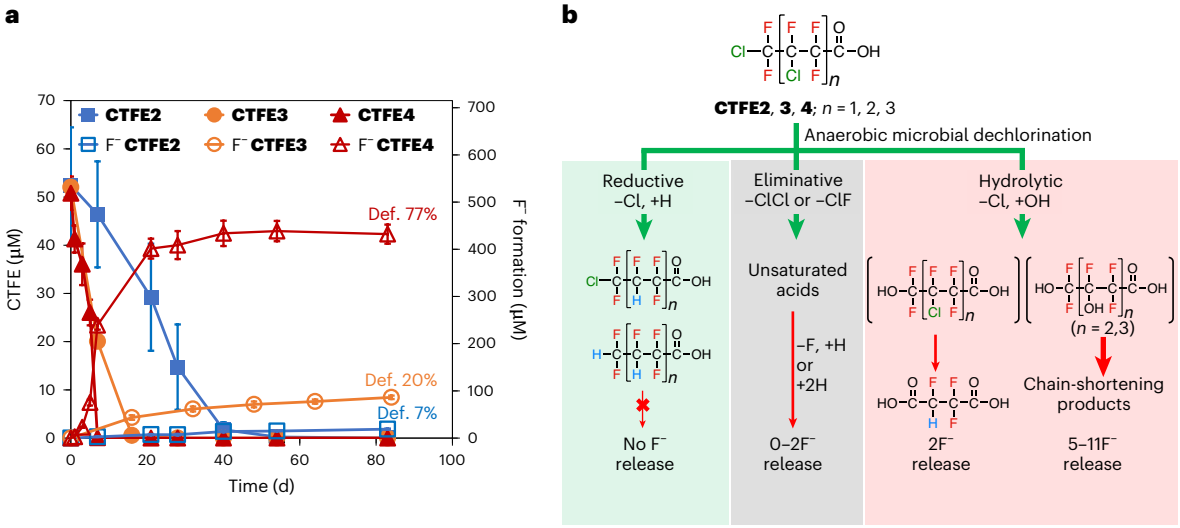

Fig. 1 | Biotransformation and defluorination pathways of CTFE oligomer carboxylic acids by the anaerobic microbial community. a, Parent compound decay and F^- formation over 84 days. The data are presented as mean values. The error bars represent the s.d. from $n = 3$ replicate experiments. Def., defluorination. **b**, The proposed general biotransformation pathways. Green arrows represent dechlorinating reactions. Red arrows represent defluorinating reactions. The thickness of the red arrows represents the number of F^- ions released. The green-shaded panel shows the non-defluorinating reductive dechlorination pathway (−Cl, +H). The grey-shaded panel shows the defluorinating pathway via eliminative dechlorination (−ClCl or −ClF). The pink-shaded panel shows the defluorinating pathway via hydrolytic dechlorination (−Cl, +OH). Note that aerobic biotransformation or abiotic transformation was not observed, except for a minor release of fluoride from **CTFE4** in the heat-inactivated sludge controls, perhaps due to some remaining biological activity (Supplementary Figs. 1 and 2j–l).

not well documented. Studies on the transformations of Cl-PFAS by microbes and higher organisms have been limited to certain structures, with reductive dechlorination being the major reported biotransformation pathway[29–31]. Whether and how environmental microbes defluorinate other important Cl-PFAS, such as CTFE oligomer acids, and how the number and position of Cl substitutions would affect biodegradability are as yet unknown.

Here we report the enhanced anaerobic microbial biotransformations of a comprehensive set of environmentally important Cl-PFAS (Supplementary Tables 1 and 2) by three types of dechlorination reaction. We demonstrate that hydrolytic dechlorination triggers substantial defluorination of CTFE trimer and tetramer acids by elucidating the biotransformation and biodefluorination pathways. We interpret the structure–biodegradability relationship and identify the responsible microorganisms. The findings offer new insights into the environmental fate of Cl-PFAS, particularly the CTFE oligomer acids, PFAS source tracking, the design of readily biodegradable alternative PFAS and the development of cost-effective biotechnologies for the clean-up of PFAS from impacted environments.

Results

Dechlorination-induced defluorination of CTFE oligomer acids

All three CTFE oligomer carboxylic acids (that is, **CTFE2**, **CTFE3** and **CTFE4**; for structures, see Fig. 1b) investigated in this study were completely biotransformed with substantial fluoride release by the sludge community under anaerobic conditions. With increasing Cl substitutions in the structure from the dimer to tetramer acid, the half-life decreased from 19 to 3 days (Supplementary Table 3), and the degree of defluorination increased significantly (Student's t-test, $P < 0.05$) from <10% to ~80% after 84 days (Fig. 1a). Transformation product (TP) analysis indicated that the three CTFE oligomer acids first underwent microbial dechlorination reactions, including reductive, hydrolytic and eliminative dechlorination. The hydrolytic dechlorination reaction triggered substantial defluorination (Fig. 1b), which was more favourable for the trimer and tetramer acids that have more Cl substitutions, leading to more defluorination. Reductive dechlorination gave TPs that were more recalcitrant to biotransformation and did not undergo defluorination. Eliminative dechlorination led to the formation of unsaturated TPs, some of which underwent much slower reductive defluorination or hydrogenation as reported previously[19], contributing the release of zero to two F^-. Stable unsaturated TPs with multiple C=C bonds caused the dark-yellow colour that developed during the defluorination of **CTFE4**.

The hydrolytic dechlorination reaction produced unstable fluoroalcohol moieties that underwent spontaneous HF elimination. The acyl fluoride structure resulting from hydrolytic dechlorination at the terminal position could be further hydrolysed, resulting in a diacid, such as TP170 in the case of the CTFE dimer acid **CTFE2** (Fig. 2b). Two F atoms were cleaved per molecule of TP170 formed in this defluorinating pathway. The theoretical release of F^- (15.8 μM), corresponding to the 7.9 μM TP170 formed on day 192 (Fig. 2a), was less than the actual total release of F^- (26 μM) from **CTFE2**, probably due to the formation of undetected defluorination intermediates such as chlorotrifluorosuccinic acid, as indicated in Fig. 2b. Assuming that two F^- would be released per parent compound molecule via the defluorinating pathways, the actual total release of 26 μM F^- would correspond to 13 μM of the initial 52 μM **CTFE2** (Fig. 2a). Thus, the remaining **CTFE2** (39 μM, 75%) underwent non-defluorinating pathways, that is, reductive and eliminative dechlorination (Fig. 2b) to form more recalcitrant TPs that exhibited slower (TP210 and TP174) or no biotransformation/defluorination (TP176; Fig. 2a).

The biotransformation became faster with increasing number of CTFE monomers in the oligomers. All three types of dechlorination reaction also occurred with the trimer and tetramer acids (**CTFE3** and **CTFE4**, respectively), as indicated by the detected TPs, with the anaerobic hydrolytic dechlorination and spontaneous defluorination pathway more favoured as more diacid TPs were formed (Fig. 3). Theoretical BDE calculations (Supplementary Methods) suggested that the BDEs of the C–Cl bonds in **CTFE3** and **CTFE4** are lower than those in **CTFE2** (Supplementary Fig. 4a), especially the internal C–Cl bonds. The C–Cl bonds with lower BDEs in **CTFE3** and **CTFE4** could be more

https://doi.org/10.1038/s44221-023-00077-6

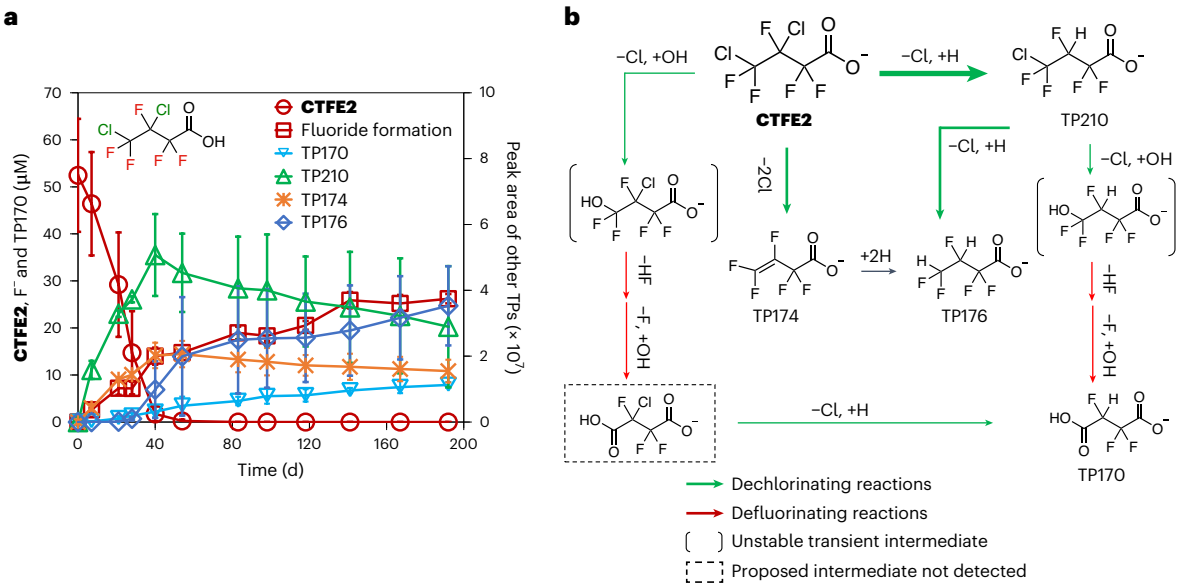

Fig. 2 | Biotransformation and defluorination pathways of CTFE2 by the anaerobic microbial community. a, The decay of **CTFE2** and the formation of fluoride and TPs. TP170 was quantified using a reference standard and is shown on the left-hand *y* axis along with F^- and the initial **CTFE2**, while the other TPs are represented as peak areas on the right-hand *y* axis. The data are presented as mean values. The error bars represent the s.d. from $n = 3$ replicate experiments. **b**, Proposed biotransformation pathways for **CTFE2**. Green arrows indicate dechlorinating reactions. Red arrows indicate defluorinating reactions. The thickness of the arrows represents the relative proportion of **CTFE2** undergoing the different pathways. Reaction code: −Cl, +H, reductive dechlorination; −2Cl, eliminative dechlorination; −Cl, +OH, hydrolytic dechlorination; −HF, eliminative defluorination; −F, +OH, hydrolytic defluorination. Unstable transient intermediates are shown in brackets. The proposed TPs not detected by liquid chromatography coupled with high-resolution mass spectrometry (LC–HRMS) are shown in dashed boxes. See Supplementary Fig. 3a–d for LC coupled with tandem HRMS (LC–HRMS/MS) detection of the four identified TPs.

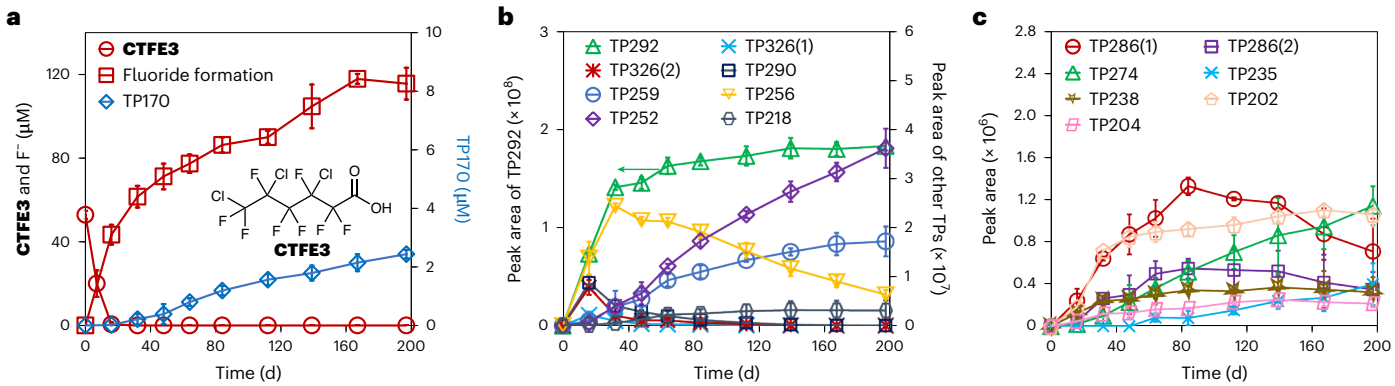

Fig. 3 | Biotransformation and defluorination of CTFE3 by the anaerobic microbial community. a, **CTFE3** decay and formation of TP170 and F^-. TP170 was quantified using a reference standard. **b**,**c**, Other TPs formed in higher (**b**) and lower (**c**) peak areas from the decay of **CTFE3**. The data presented in **b** and **c** are peak areas with different *y*-axis scales. The data are presented as mean values. (1) and (2) represent isomers of TPs with the same *m/z* value and formula but different retention times on the LC–HRMS. The error bars represent the s.d. from $n = 3$ replicate experiments.

reactive in an anaerobic microbial system, particularly in the hydrolytic dechlorination reaction, thus leading to faster biotransformation and greater defluorination.

Besides diacid TPs with the same chain length as the starting CTFE, shorter-chain diacids were also formed in the hydrolytic dechlorination pathway, including C_4 and C_5 diacids from **CTFE3** and C_3, C_4 and C_7 diacids from **CTFE4** (Fig. 3b,c and Fig. 4a,b). The longer chain with additional Cl substitutions in **CTFE3** and **CTFE4** likely allows hydrolytic dechlorination to occur at multiple Cl substitution sites in the middle of the structure either simultaneously or in series. Fluoro keto acids ($RCO(CH_2)_nCOOH$, $n = 0, 1, 2$) may also be formed, as a fluoro keto acid was detected as a transient intermediate from **CTFE4** (TP404 in Supplementary Fig. 5e,g). The fluoro keto acids, if formed, would be unstable and undergo chain-shortening reactions to yield the detected shorter-chain acids or diacids (reaction (v) in Fig. 4a). α-Keto diacids were decarboxylated, forming one-carbon-shortened TPs (that is, TP202 and TP370 from **CTFE3** and **CTFE4**, respectively; Fig. 4a,b). The C_7 diacid TP370 was a major intermediate of **CTFE4** (Supplementary Fig. 5b,g), and was further transformed, likely via hydrolytic dechlorination at either of the two Cl substitutions, forming C_7 β-keto fluoro diacids. C_6 and C_8 β-keto fluoro diacid intermediates were also proposed to form from **CTFE3** and **CTFE4**, respectively (Fig. 4a,b). These structures are unstable and subject to hydrolysis. Furthermore, the microbial decomposition of β-keto acids to form acetate and the

https://doi.org/10.1038/s44221-023-00077-6

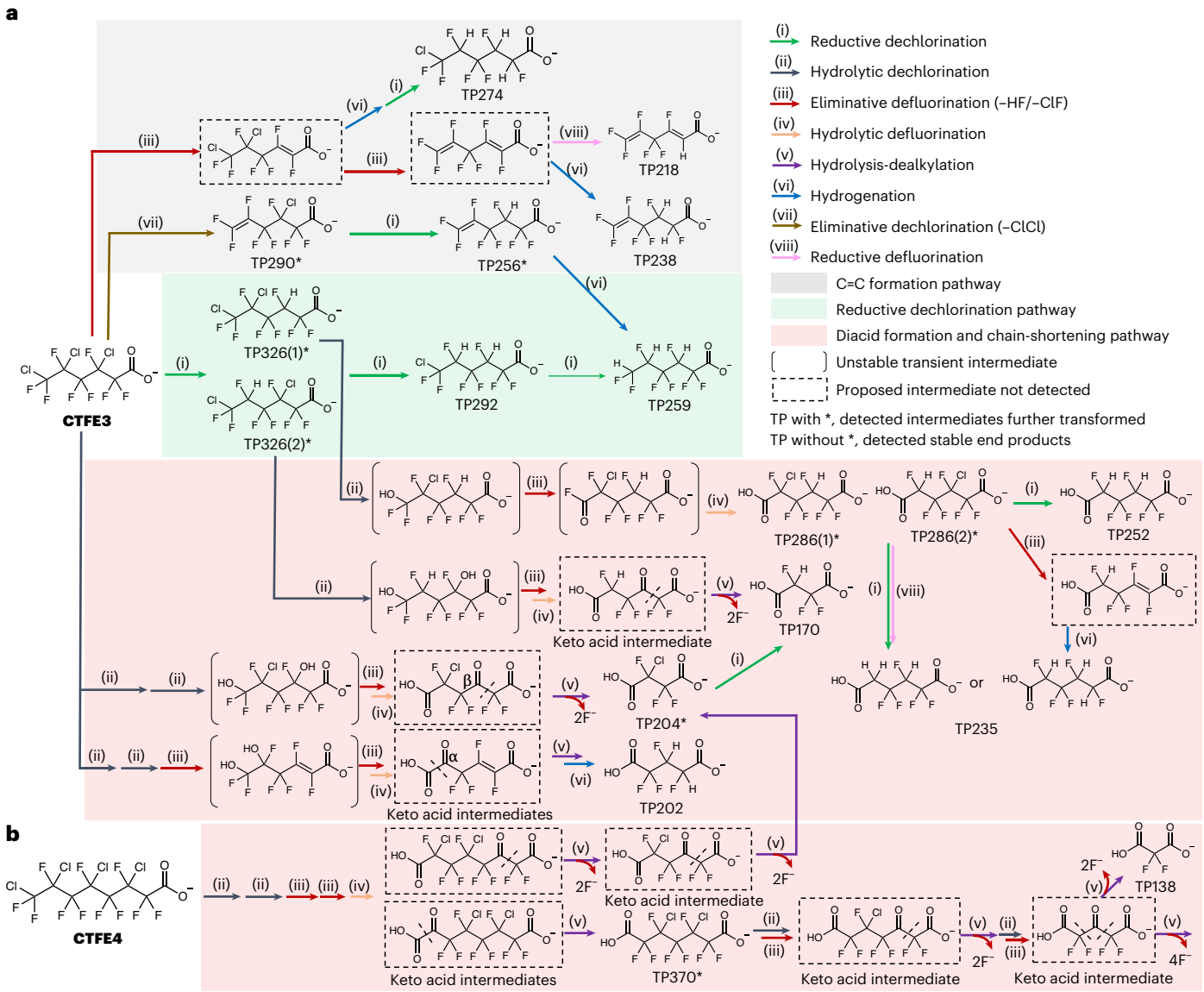

Fig. 4 | Proposed biotransformation pathways for CTFE3 and CTFE4. **a**,**b**, Proposed pathways for **CTFE3** (**a**) and the proposed key defluorination pathways via hydrolytic dechlorination and chain-shortening reactions for **CTFE4** (**b**). See Supplementary Fig. 5a–f for the TP formation curves of **CTFE4**, and Supplementary Figs. 3e–p and 5g for the LC–HRMS/MS detection of the identified TPs of **CTFE3** and **CTFE4**, respectively.

corresponding C_{n-2} acid has been reported[32]. However, difluoroacetate was not detected in our analysis, indicating that it was not formed from the chain-shortening reaction as it is recalcitrant to anaerobic defluorination (Supplementary Fig. 6) and would have accumulated and been detected if formed. Two alternative scenarios were proposed: a carbene ($:CF_2COO^-$) formed during C–C cleavage, followed by the formation of CO with F^- release, similar to the transformation of $CFCl_3$ in the anaerobic iron porphyrin–cysteine system[33], or a hydroxy group attached to the leaving group, followed by spontaneous defluorination. C_5 and C_6 diacids from the deacetylation of the C_7 and C_8 β-keto fluoro diacids were not detected, indicating that further transformation was likely via hydrolytic dechlorination at the remaining Cl substitution sites, forming C_5 and C_6 β-keto diacid intermediates (Fig. 4b). The C_5 β-keto diacid in Fig. 4b could then be cleaved at two symmetric positions, leading to complete defluorination, or at one position to form the stable difluoromalonic acid (TP138, structure confirmed in Supplementary Fig. 5h), a TP unique to **CTFE4**. The C_6 β-keto diacid may form a C_4 diacid, that is, chlorotrifluorosuccinic acid (TP204), which was also a deacetylation product from **CTFE3** (Fig. 4a). Chlorotrifluorosuccinic acid (TP204) underwent a very slow biotransformation to trifluorosuccinic acid (TP170; the structure confirmed is in Supplementary Fig. 3d) via reductive dechlorination (Figs. 3a and 4a). This suggests that hydrolytic dechlorination is more difficult for C–Cl bonds in C_3 and C_4 fluoro diacids.

We then identified the major pathways leading to defluorination in the biotransformations of **CTFE3** and **CTFE4**. For the quantifiable less fluorinated TPs, trifluorosuccinic acid (TP170) and difluoromalonic acid (TP138) accounted for less than 10% (1.5–3 μM formation each) of the initial parent compound, indicating that they were not the major end products and that their formation pathways were not the major routes. Instead, for **CTFE3**, the formation of C_6 diacids (for example, TP252) with the release of two F^- via the hydrolytic dechlorination pathway was more likely the major defluorination route. The greater defluorination (release of three to five F^-) from chain-shortening pathways and the lower defluorination (release of no or just one F^-) from the reductive and eliminative dechlorination pathways averaged out to 27% of the observed defluorination of **CTFE3** (release of about two of the eight F atoms per added molecule) on the last day of incubation

https://doi.org/10.1038/s44221-023-00077-6

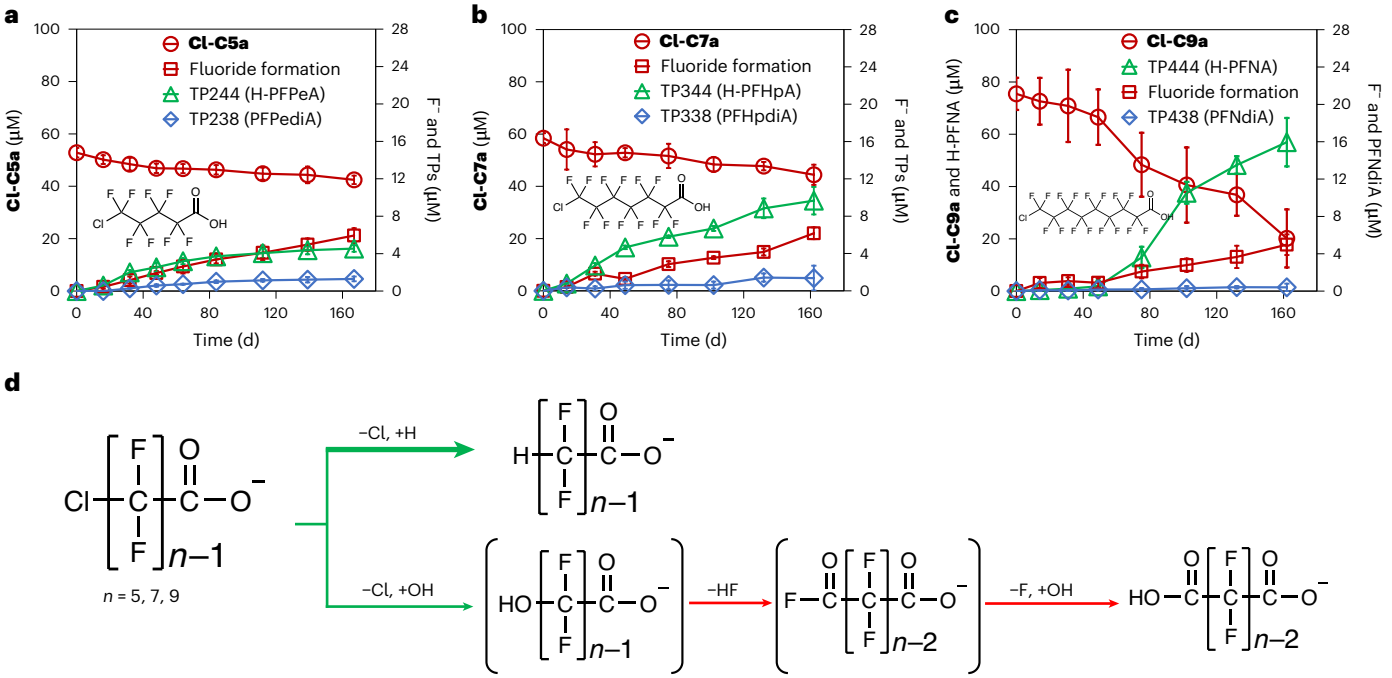

Fig. 5 | Biotransformation of Cl-terminal PFCAs by the anaerobic microbial community. a–c, Parent compound decay, F^- release and TP formation from **Cl-C5a** (**a**), **Cl-C7a** (**b**) and **Cl-C9a** (**c**). The data are presented as mean values. The error bars represent the s.d. from $n = 3$ experimental replicates. **d**, The proposed biotransformation pathways shared by **Cl-C5a**, **Cl-C7a** and **Cl-C9a**. Red arrows represent defluorinating reactions. Green arrows represent dechlorinating reactions. Unstable transient TPs are shown in brackets. No aerobic or abiotic transformation or adsorption was observed, as shown in Supplementary Figs. 1 and 2g–i. See Supplementary Fig. 9 for the LC–HRMS/MS detection of the identified TPs.

(day 197). Similarly, according to the 77% total defluorination of **CTFE4** after ~200 days, an average of 8 to 9 of the 11 F atoms should be released per added **CTFE4** if all underwent defluorination. As **CTFE4** partially underwent reductive and eliminative dechlorination pathways with no or much lower F^- release, we reasonably expect that a substantial portion of **CTFE4** underwent complete defluorination and propose a pathway via the formation of the C_7 diacid TP370, as shown in Fig. 4b.

Dechlorination-enhanced defluorination of other polyfluorocarboxylic acids

The biotransformation of other environmentally relevant Cl-PFCAs, such as Cl-terminal and ultra-short-chain structures, was also significantly (Student's *t*-test, $P < 0.05$) stimulated compared with their H-substituted counterparts, which exhibited no or very little biotransformation (Figs. 5a–c and 6a,b and Supplementary Figs. 6, 7 and 8a,b). The enhanced biodegradability was attributed to biodechlorination pathways similar to those of the CTFE oligomer acids. In contrast to the polychlorinated structures (that is, CTFE oligomer acids and dichlorofluoro C_2 and C_3 acids), which showed complete and fast biotransformation and defluorination (Figs. 1a and 6a,b), the biotransformations of monochlorinated structures (that is, Cl-terminal polyfluorocarboxylic acid (PFCAs) and monochloro-perfluoro C_2 and C_3 acids) was much slower (Supplementary Table 3). The biotransformation was incomplete after more than 160 days for the Cl-terminal C_5, C_7 and C_9 PFCAs (Fig. 5a–c), and the Cl-terminal C_2 and C_3 PFCAs did not show any biotransformation (Supplementary Fig. 6). This is in line with the much higher BDE of the terminal C–Cl bond in those structures (Supplementary Fig. 4b,c).

All three C_5, C_7 and C_9 biotransformed Cl-terminal PFCAs share two common biotransformation pathways, namely the major non-defluorinating reductive dechlorination pathway and the minor defluorinating hydrolytic dechlorination pathway, the same as for the CTFE oligomer acids (Fig. 5d). The reductive dechlorination of the parent compound increased with chain length (Fig. 5a–c). More than half of **Cl-C9a** was reductively dechlorinated, while less than 25% of the C_5 and C_7 structures underwent the same process. Reductive dechlorination has been reported as the major biotransformation pathway for other Cl-terminal PFAS structures, such as 8:2 chlorinated polyfluorinated ether sulfonate (8:2 Cl-PFESA) and 6:2 Cl-PFESA (F-53B), which were not defluorinated[29–31]. It is worth noting that notable active biosorption (~60%) was observed for **Cl-9a** ($n = 9$), while the tested structures with a chain length of $n \leq 8$ showed less than 5% adsorption to biomass. **Cl-9a** was only taken up by actively growing biomass (Supplementary Fig. 10), and not by heat-inactivated biomass (Supplementary Fig. 2i). The active biosorption of its two TPs, that is,H-terminal perfluorononanoic acid (H-PFNA) and perfluorononanoic diacid (PFNdiA), was much lower (10–13%; Supplementary Fig. 10), suggesting that the biotransformation of less mobile PFAS can result in TPs with higher mobility, thus being more easily transported into aqueous environments.

Compared with **Cl-C3a** with terminal Cl substitution, which did not exhibit any biotransformation, **Cl-C3b** (2-chloro-2,3,3,3-tetrafluoropropanoic acid) with α-Cl substitution showed a much faster and complete biotransformation (Fig. 6d), but without defluorination (Fig. 6b). It was reductively dechlorinated to form the stable TP144 (2,3,3,3-tetrafluoropropanoic acid (**C3b**); Fig. 6g). This agrees with the lower BDE of the α-C–Cl bond in **Cl-C3b** compared with the terminal C–Cl bond in **Cl-C3a** (Supplementary Fig. 4c) and again suggests that C–Cl bonds closer to the carboxy group are more reactive.

The reductive dechlorination product (TP144, **C3b**) accounted for 90% of the added **Cl-C3b**, with the formation of 3,3,3-trifluoropropionate (TP127, **C3c**) accounting for the remaining 10% (~6 μM; Fig. 6d). **C3c** is the reductive dehalogenation product of **Cl-C3b** (that is, Cl→H and F→H). As the Cl→H product **C3b** did not undergo further biotransformation, the F→H exchange most likely occurred at the same time as the reductive dechlorination. The formation of **C3c** (2–3 μM after 64

https://doi.org/10.1038/s44221-023-00077-6

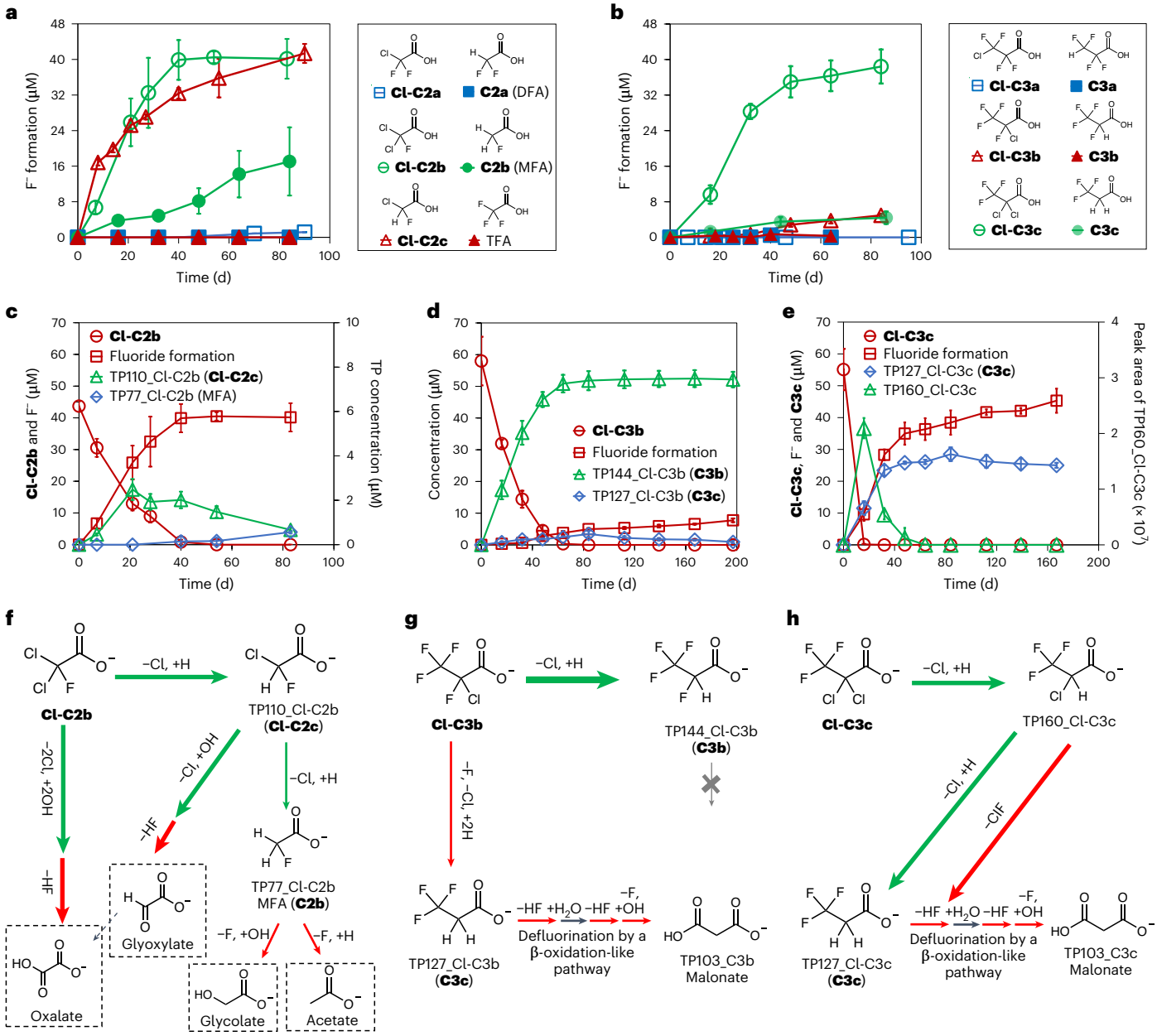

Fig. 6 | Biotransformation of C_2 and C_3 chlorinated fluorocarboxylic acids and their H-substituted counterparts by the anaerobic microbial community. **a**,**b**, Defluorination of C_2 (**a**) and C_3 (**b**) chlorinated fluorocarboxylic acids. The initial concentration of the parent compounds was 50 μM. Except for **Cl-C2c**, which showed abiotic and aerobic defluorination, none of the other compounds was abiotically or aerobically transformed, as shown in Supplementary Figs. 1 and 2a–f. MFA, monofluoroacetic acid; DFA, difluoroacetic acid; TFA, trifluoroacetic acid. **c**–**e**, Parent compound removal, F^- release and TP formation from **Cl-C2b** (**c**), **Cl-C3b** (**d**) and **Cl-C3c** (**e**). In **a**–**e**, the data are presented as mean values. The error bars represent the s.d. from $n = 3$ experimental replicates. **f**–**h**, The proposed biotransformation pathways of **Cl-C2b** (**f**), **Cl-C3b** (**g**) and **Cl-C3c** (**h**). Note that no F^- formation was observed for the three compounds in abiotic and heat-inactivated sludge controls, with the exception of **Cl-C3c**, which underwent a non-defluorinating abiotic transformation (Supplementary Fig. 2b,e,f). Red arrows represent defluorinating reactions. Green arrows represent dechlorinating reactions. The thickness of the arrows represent the relative proportion of **Cl-C2b** (**f**), **Cl-C3b** (**g**), and **Cl-C3c** (**h**) undergoing the different pathways. Proposed TPs whose formation was difficult to determine because of potential formation from other essential metabolic routes and their further use during anaerobic growth are shown in dashed brackets. In **f**, two possible reaction pathways for MFA are presented, namely hydrolytic defluorination (−F, +OH)[46] and reductive defluorination (−F, +H)[47]. The 'β-oxidation-like pathway' is the same as that reported in a previous study[34]. See Supplementary Fig. 11 for the LC–HRMS/MS detection of the identified TPs.

days) resulted in an equal molar concentration (2–3 μM) of F^- release (Fig. 6d,g). **C3c** was very slowly defluorinated anaerobically (Fig. 6b), leading to a further small increase in released F^- after the depletion of **Cl-C3b** (Fig. 6d). The anaerobic defluorination of **C3c** occurred via the same β-oxidation-like pathway as its aerobic defluorination[34]. This is supported by the increase in malonate, the end product of this pathway (Supplementary Fig. 7a). The reductive dechlorination of 2,2-dichloro-3,3,3-trifluoropropanoic acid (**Cl-C3c**) also led to the formation of **C3c**, but the slow defluorination of **C3c** could not contribute to the rapid release of F^- from **Cl-C3c** observed within 40 days (Fig. 6e,h). Instead, the primary reductive dechlorination product TP160 seemed to partially undergo eliminative dehalogenation (−ClF; Fig. 6h), leading to a 1:1 release of F^-. The −ClF product, an intermediate of the **C3c** biodefluorination pathway, was not detected and might be

https://doi.org/10.1038/s44221-023-00077-6

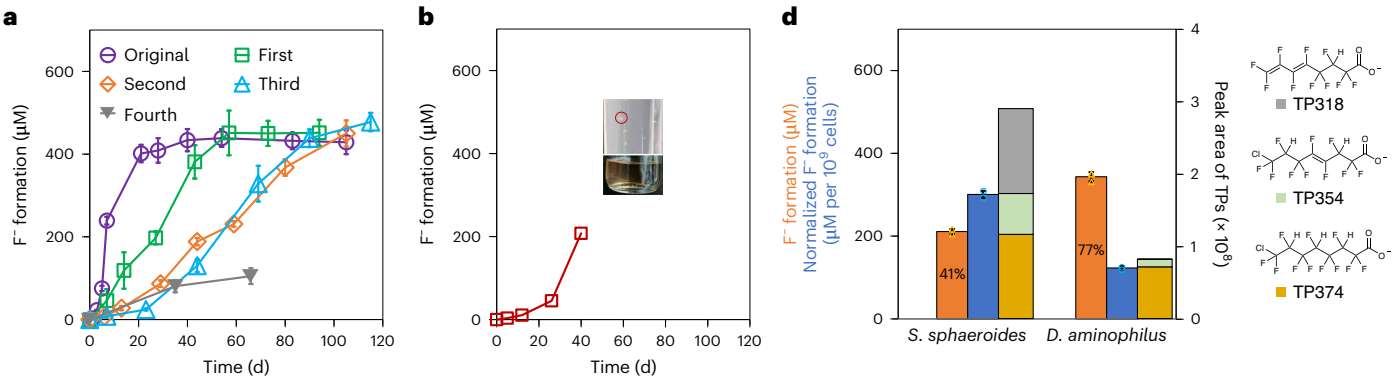

c

Bin-genome	Closest genome	Similarity (coverage) (%)	Relative abundance (%)	RDH	HAD	HAD family hydrolases	Dissimilatory sulfate reduction pathway
Bin 1	*S. sphaeroides*	97.3 (81)	35.8	0	0	1	–
Bin 2	*D. aminophilus*	92.0 (81)	49.0	0	0	1	+

Fig. 7 | CTFE4 defluorination in subcultures of the anaerobic communities, the isolated colony and the pure cultures. a, Defluorination of 50 μM **CTFE4** in subcultures of anaerobic communities. The data are presented as mean values. The error bars represent the s.d. from $n = 3$ experimental replicates, except for the fourth subculture, the error bars of which represent the s.d. from $n = 2$ experimental replicates. **b**, Defluorination of 50 μM **CTFE4** in the colony isolated from the third subculture. The upper photo in the inset shows the morphology of the isolated colony, and the lower photo shows the liquid culture of the isolated colony after 40 days' growth. **c**, Characteristics of the two major genomes reconstructed from the metagenome of the isolated colony. HAD family hydrolases includes a variety of hydrolases, including 2-haloacid dehalogenases. **d**. Total fluoride formation, cell-normalized fluoride formation and the major stable TPs from **CTFE4** (50 μM) formed in *S. sphaeroides* and *D. aminophilus* after 40 days. The data are presented as mean values. The error bars represent the s.d. from $n = 2$ experimental replicates for *S. sphaeroides* and $n = 3$ experimental replicates for *D. aminophilus*. The dot plots represent the raw data for total fluoride formation (yellow triangles) and cell-normalized fluoride formation (blue circles). The average total defluorination percentage is indicated in the first column. Representative isomeric structures of TP354, TP354 and TP318 are shown (right). See Supplementary Fig. 5g for all possible isomeric structures.

further transformed. This pathway led to a slower release of F^- after the depletion of TP160 (Fig. 6e,h).

It is likely that the two C_2 acids 2,2-dichloro-2-fluoroacetate (**Cl-C2b**) and its primary reductive dechlorination product 2-chloro-2-fluoroacetate (**Cl-C2c**) underwent hydrolytic dechlorination, triggering the nearly complete defluorination (Fig. 6a,c,f). The reductive dechlorination product TP77 (2-fluoroacetic acid) of **Cl-C2b** and **Cl-C2c** was detected at a low level, and its defluorination was slow (Fig. 6a,c and Supplementary Fig. 7). Thus, the fast and complete defluorination should be triggered by the hydrolytic dechlorination of **Cl-C2b** and **Cl-C2c**. It was reported previously that di- and monochloroacetate were converted into glyoxylate by a haloacid dehalogenase in an anaerobic bacterium '*Candidatus* Dichloromethanomonas elyunquensis' strain RM via hydrolytic dechlorination[35]. Thus, it is possible that the structurally similar **Cl-C2b** and **Cl-C2c**, with one C–H replaced by C–F, can also undergo hydrolytic dechlorination in an anaerobic microbial community, leading to spontaneous cleavage of the C–F bond.

Microorganisms responsible for the defluorination of CTFE4

So far we have demonstrated substantial defluorination triggered by hydrolytic dechlorination of various Cl-PFCAs. We next focused on **CTFE4,** which exhibited the greatest defluorination, and tried to enrich the responsible microorganisms. However, during the enrichment process, the defluorination rate of **CTFE4** decreased after subculturing four times, that is, transferring 5% (v/v) of the previous culture into the same basal medium amended with 123 mM methanol and 50 μM **CTFE4** (Fig. 7a). This suggests that the dehalogenation of **CTFE4** does not support or benefit the sustainable growth of the responsible microorganisms, rendering diluted biomass and decreasing defluorination activity. As **CTFE4** dehalogenation did not lead to outgrowth of the responsible microorganisms, cultivation-independent metagenomic analysis would not provide clear clues as to the identity of the responsible microorganisms, as the abundant species would most likely be those grown by methanol fermentation without **CTFE4** dehalogenation.

Therefore, we used the isolation approach to identify responsible microbes. From the third subculture, we isolated and screened one colony that exhibited a similar **CTFE4** defluorination activity as the third subculture in the same medium after 40 days (Fig. 7b). It was a highly enriched culture consisting of two dominant bingenomes that were most similar to the genomes of *Sporomusa sphaeroides* and *Desulfovibrio aminophilus* (Fig. 7c and Supplementary Table 4). We then obtained pure cultures of *S. sphaeroides* (DSM 2875) and *D. aminophilus* (DSM 12254), which completely removed **CTFE4** after 21 and 14 days, respectively (Supplementary Fig. 12). The total defluorination was about twofold higher in *D. aminophilus* (77%) than in *S. sphaeroides* (41%; Fig. 7d). The faster removal and greater defluorination of **CTFE4** in *D. aminophilus* can be attributed to its faster growth compared with *S. sphaeroides*, while the latter showed a higher (2.4-fold) defluorination capacity per cell. Additionally, *S. sphaeroides* converted more **CTFE4** into stable, less defluorinated products via reductive and eliminative dechlorination (Fig. 7d), and this could also result in the lower total defluorination compared with in *D. aminophilus*. Given the phylogenetically insignificant similarity of the two identified genomes to the two tested pure strains, as well as the phylogenetic divergence between the two genomes, **CTFE4**-degrading microorganisms might be less specific across the same genus and commonly occurring in anaerobic environments. Knowing the characteristics of the defluorinating microorganisms could help to enhance defluorination in a microbial

community. Given that the *Desulfovibrio*-like bingenome possesses dissimilatory sulfate reduction pathways (Supplementary Fig. 8c)[36], by providing sulfate to the fourth subculture of the **CTFE4**-defluorinating microcosm with declined defluorination activity (Fig. 7a), we selectively stimulated the growth of the defluorinating sulfate reducers in the community, thus substantially boosting the defluorination of **CTFE4** (Supplementary Fig. 13). Neither of the two bingenomes has genes annotated as reductive dehalogenases (RDHs) or 2-haloacid dehalogenases (HAD; Fig. 7c). Only one HAD family hydrolase gene with unclear specific function was annotated in the two bingenomes with 40% amino acid similarity. Whether the HAD family protein could catalyse the hydrolytic dechlorination of **CTFE4** remains unclear and warrants future investigation.

Implications for PFAS research

Polytetrafluoroethylene (PTFE) and PCTFE are two widely used fluoropolymers. Compared with polytetrafluoroethylene, PCTFE, with one F substituted by Cl in the CTFE monomer, would become more biodegradable and less persistent in the environment once transformed into CTFE oligomer carboxylic acids via thermal decomposition[9–11] or oxidative metabolism[12,13]. Our findings also indicate that longer-chain CTFE oligomer acids may have an even shorter half-life and undergo much greater defluorination in anaerobic environments where the identified responsible microorganisms (*Desulfovibrio* and *Sporomusa* species) are commonly distributed[37–40]. It is worth noting that despite the enhanced bioavailability of the Cl-substituted structures, only specific types of dechlorination, namely hydrolytic and eliminative dechlorination, can trigger the defluorination of CTFE oligomer acids. The importance of previously underestimated non-respiratory hydrolytic dechlorination genes in chlorinated natural organic matter cycling was recently highlighted, given their high detection frequencies in the environment[37]. Here, we have demonstrated another critical role that they may play in the defluorination of chlorinated PFAS.

The higher biodegradation potential of chlorinated PFAS could provide critical guidance for the design of alternative PFAS that are more readily biodegradable and meanwhile have similar functionality and no increase in toxicity. It is commonly thought that an increase in the number of Cl substitutions could render higher toxicity. This seems not to be the case with regards the microbial toxicity of chlorinated PFAS. The mono- and poly-Cl-PFCAs (C_4 to C_9) investigated in this study showed a lower inhibitory effect than PFCAs with the same chain length on the luminescence of *Vibrio fischeri* (Supplementary Fig. 14), the standard toxicity measurement[41]. In contrast, the H-terminal PFCA, a major biotransformation product of the corresponding Cl-terminal PFCA, exhibited a higher inhibitory effect on the luminescence than the parent compound. It should be noted that the luminescent bacteria test only indicates acute microbial toxicity. Toxicity tests using higher organisms are needed to obtain a comprehensive and systematic evaluation of the ecotoxicity of chlorinated PFAS.

Another concern might be that although Cl substitutions enhanced biodegradability, complete defluorination was still not achieved due to non-defluorinating biotransformation pathways, such as the reductive dechlorination pathway. The incompletely defluorinated products might be more mobile in the aquatic environment with higher toxicity to the ecosystem. Nonetheless, as many of them contain C–H bonds at saturated and unsaturated carbon atoms, they are prone to aerobic biodegradation, as indicated in our previous studies[20,34]. We collected the spent medium of cultures after reaching maximum anaerobic defluorination (~80%) of the CTFE tetramer acid and further treated it aerobically using the activated sludge community collected from the same wastewater treatment plant (WWTP). An additional 12% defluorination was achieved after 9 days (Supplementary Fig. 15). Therefore, a sequential anaerobic–aerobic bioreactor could be adapted from the anaerobic–aerobic configurations commonly employed in municipal or industrial wastewater treatment by increasing the anaerobic sludge retention time to cost-effectively treat wastewater containing CTFE tetramer acid. Nearly complete destruction of the tetramer acid that enters aquatic environments may also be expected at the anaerobic–aerobic interface in nature.

The novel biotransformation pathways identified for Cl-PFCAs also provide important insights into PFAS source tracking, environmental monitoring and risk assessment. Besides the reported H-terminal polyfluorocarboxylic acids from reductive dechlorination, two new groups of TP, that is, perfluorodicarboxylic acids and unsaturated fluorocarboxylic acids, have been demonstrated experimentally from the anaerobic biotransformation of various Cl-PFCAs. Thus, Cl-PFAS could be a critical source of all three of the above classes of emerging PFAS detected in different environments[25,42]. This is supported by recent studies[25,43] that revealed correlations between the detection of H-substituted, unsaturated and diacid products and the occurrence of Cl-PFAS in impacted wastewater and soils. Thus, closer and more accurate PFAS monitoring and toxicity studies could also be conducted on the non- and slowly biotransformed Cl-PFAS as well as the stable end products (for example, H-terminal polyfluorocarboxylic acids, perfluorodicarboxylic acids and unsaturated PFCAs) given their persistence in the aquatic environment.

The discovery of the new capabilities of commonly occurring anaerobic microorganisms in transforming and defluorinating industrially critical Cl-PFAS not only advances the current fundamental knowledge of microbial dehalogenation, but also provides critical insights into a more accurate assessment of the environmental fate and ecotoxicity of Cl-PFAS, the design of readily biodegradable and less toxic alternative PFAS, and the development of cost-effective bioremediation strategies.

Methods

Chemicals

The 12 Cl-PFCAs (see Supplementary Table 1 for details) investigated in this study were purchased from SynQuest Laboratories, Matrix Scientific and Manchester Organics. Stock solutions (~10 mM) of individual Cl-PFCAs and reference compounds of plausible TPs (Supplementary Table 2) were prepared in methanol (HPLC grade). All the stock solutions were stored at −20 °C.

Anaerobic biotransformation

An activated sludge community freshly taken from a local municipal WWTP was used. To avoid the carryover of dissolved oxygen, settled activated sludge (6,700–6,800 mg suspended solids per litre) was inoculated (10%, v/v) into a 160-ml sealed serum bottle containing 90 ml autoclaved basal medium containing vitamins, including 100 μg l^{-1} B_{12}, as previously described[44], and a 60-ml headspace of Ar/CO_2 (75:25, v/v). Methanol (~123 mM), as an electron donor, was added to the culture and re-added twice a week. The selected PFAS (~50 μM) was spiked into the culture. The pH of the culture was buffered at 7.4 ± 0.1. Biomass-free abiotic and heat-inactivated biomass controls were prepared in the same way using autoclaved sludge filtrate (0.22 μm) and autoclaved sludge instead of the activated sludge as the inoculum, respectively. Sodium azide was added (~0.2 g l^{-1}) to both abiotic and heat-inactivated biomass controls to further inhibit microbial activities over the entire incubation period. All cultures were incubated in the dark at 34 °C without shaking. The biotransformation experiments with the activated sludge communities and abiotic and heat-inactivated controls were performed in triplicate. One bottle containing only sludge was also studied as a control for the sludge matrix, which was subtracted in the TP analyses.

Samples (2 ml) were removed periodically and centrifuged at 16,000*g* at 4 °C for 35 min. The supernatant was collected to measure fluoride, parent compound and TP content by the following method. Cell pellets were collected and extracted using 1 ml methanol with 0.1% NH_4OH. The ^{13}C-labelled perfluoro-n-octanoic acid-1-^{13}C

(CAS#: 864071-09-0) surrogate was spiked to account for the extraction recovery. The samples were vortexed and ultrasonicated for 30 min, and then centrifuged at 16,000*g* at 4 °C for 35 min. The concentrations of the parent compounds and TPs in the extracted samples were analysed to account for biomass adsorption. Except for **Cl-C9a**, which showed substantial biological adsorption, all tested Cl-PFCAs showed less than 5% adsorption by the biomass. Thus, extracellular concentrations of the parent compounds and TPs were used to interpret biotransformation pathways, except for **Cl-C9a** and its TPs, for which the total concentrations (extracellular and biomass-associated) were used. The half-lives of the parent compounds were determined assuming first-order reaction kinetics (see Supplementary Methods for details).

Aerobic biotransformation

The aerobic biotransformation experiments were conducted using a similar set-up to that used in a previous study[34]. Thus, 50 ml of fresh activated sludge (~4,400 mg l^{-1} as total suspended solids) was inoculated into batch reactors (150 ml, loosely capped) spiked with ~50 μM Cl-PFCA and incubated with shaking (150 r.p.m.) at room temperature for 5 days. The level of dissolved oxygen in the reactors was measured and remained at 4–5 mg l^{-1} over the period of study. Heat-inactivated controls were prepared using autoclaved (121 °C, 40 min) sludge and autoclaved sludge filtrate (0.22 μm filter). A sludge-only control was also analysed to obtain the F^- concentration in the sludge matrix, which did not show any notable change throughout the incubation period.

Fluoride measurement

The F^- concentration was measured using an HQ30D portable multimeter (HACH) connected to an ion-selective electrode (HACH) with a limit of quantification of 0.01 mg l^{-1} (~0.5 μM). First, 0.1 g fluoride ionic strength adjustor powder (HACH) was dissolved in 2 ml of sample. Calibration was conducted by preparing a calibration curve using three standard sodium fluoride solutions (0.5, 1 and 2 mg l^{-1}, HACH). Calibration was conducted before each sample measurement. Samples were diluted to the calibration range, as needed, before measurement. The fluoride measurement was cross-validated by ion chromatography (Supplementary Methods). F^- formation was calculated by subtracting the F^- concentration at time zero t_0 from that at time t. The degree of defluorination was determined using the following equation.

$$\text{Degree of defluorination (\%)} = \frac{\text{F}^- \text{ formed (μM)}}{\text{Removed concentration(μM)} \times \text{Number of F in one molecule}} \times 100\%$$

Ultra-high-performance LC–HRMS analysis

All organofluorines were analysed by ultra-high-performance (UHP) LC-HRMS/MS (Q Exactive Plus, Thermo Fisher). For the UHPLC, the mobile phase consisted of 10 mM ammonium acetate in Milli-Q water (eluent A) and 10 mM ammonium acetate in HPLC-grade methanol (eluent B). A 2 μl sample was loaded onto a Hypersil Gold column (particle size 1.9 μm, 2.1 mm × 100 mm, Thermo Fisher) and eluted at a flow rate of 300 μl min^{-1}. A linear elution gradient was used: 95% A for 0–1 min, 95–5% A for 1–6 min, 5% A for 6–8 min and 95% A for 8–10 min. For HRMS, negative electrospray ionization was used for sample ionization with a default charge of one. The mass analyser was set up for both a full mass spectrometry (MS^1) scan (m/z = 50–750) at a resolution of 140,000 @ m/z = 200 and a data-dependent tandem MS (MS^2) scan at a resolution of 17,500 @ m/z = 200 with a normalized collision energy of 25.

The peak areas of all parent compounds and TPs were determined using TraceFinder 4.1 EFS and Freestyle 1.6 (Thermo Fisher). Mass spectrometry data, including MS^1 and MS^2, were primarily collected with Freestyle 1.6. The concentrations of the parent compounds and TPs with reference standards were determined by establishing external calibration curves using a matrix-match calibration standard series.

TP identification and biotransformation pathway elucidation

Suspect screening was conducted using a custom-compiled suspect list that included the possible reductive defluorination and reductive dechlorination products[19]. Non-target screening was also employed for TP analysis using the modified 'Expected and Unknown Met ID Workflow' in Compound Discoverer 3.1 (Thermo Fisher). Plausible TPs were identified using the following criteria: (1) a mass tolerance of ≤5 ppm, (2) a proper peak shape with a peak area larger than 10^5, (3) an isotopic pattern score of >70, (4) a notable formation trend over time (increasing or increasing followed by decreasing), (5) not detected in the abiotic, heat-inactivated or sludge-only controls, and (6) not identified as in-source fragments[19]. The structures of the plausible TPs were further elucidated from MS^2 fragmentation profiles. For TPs with reference compounds available, the structures were confirmed by comparing the retention times and MS^1/MS^2 profiles of the TP and reference compound. The confidence levels in the TP identification were determined according to the criteria set by Schymanski et al.[45].

We proposed the most reasonable biotransformation pathways based on the following three trends: (1) the removal trend of the parent compound, (2) the formation trend of TPs with accurate formula or identified structure, and (3) the formation trend of fluoride. The three trends should be intercorrelated. For example, for biotransformation pathways that include multiple levels of reactions, the TPs from the primary reactions should exhibit a formation trend that first increases, then decreases, followed by the formation of secondary TPs. Generally, primary transient TPs peaked when most of the parent compound had been removed, then the corresponding secondary TPs started to increase substantially; the same applied for the next level of reactions. Stable products (or end products) were those with an increasing trend or an increasing trend with a plateau if the precursor was depleted. The formation of fluoride should correspond to the formation of less-fluorinated TPs.

CTFE4-defluorinating subcultures

The original **CTFE4**-defluorinating anaerobic microcosm obtained from the activated sludge was subcultured (5%, v/v) into the same basal medium containing the same concentrations of methanol and **CTFE4**. After the defluorination reached the maximum level (~80%), the last subculture was further transferred (5%, v/v) into the same medium to obtain the subsequent subcultures.

Anaerobic isolation

Anaerobic agar shake tubes were used to isolate and purify the colonies from the **CTFE4**-defluorinating subcultures. First, 10 ml sterile agar medium (0.3–0.5%, w/w) containing the same nutrients (that is, mineral salts, vitamins, methanol and **CTFE4**) as in the broth medium was added to each 20-ml sealed glass tube with an N_2 headspace. The tubes were incubated at 45–50 °C before inoculation. After the temperature of the agar medium had decreased slightly, one agar shake tube was inoculated with 1 ml of the third subculture, then gently mixed by inverting the tube several times. Then, 1 ml of the mixture was transferred to a new agar shake tube. The contents of a set of inoculated agar shake tubes with 10^{-1} to 10^{-8} serial dilution were solidified at room temperature and incubated at 34 °C. After 14 days of incubation, individual colonies were picked up using syringe needles and inoculated into new agar shake tubes for further purification. Further purified individual colonies with different morphology were picked up and transferred into the same liquid basal medium amended with methanol (~123 mM) and **CTFE4** for the defluorination activity test. The liquid cultures from two colonies that showed defluorination activity were subject to metagenomic sequencing for genomic composition analysis.

Metagenomic sequencing

Celugation at 18,000 for 20 min at room temperature. Genomic DNA was extracted using a DNeasy Blood and Tissue Kit (Qiagen) according

to the manufacturer's instructions and then sent to the Microbial Genome Sequencing Center (Pittsburgh) for sequencing (Illumina NextSeq 2000, 2 × 150 base pairs, 680 × 10^6 base-pair output).

Reconstruction of bingenomes

The draft genome assembly and binning were performed using the Department of Energy Systems Biology Knowledgebase (KBase) platform (https://www.kbase.us/). The sequencing reads of each sample were trimmed and quality-filtered using Trimmomatic v0.36 with default parameters. The clean reads were assembled into contigs using MEGAHIT v1.2.9, and the contigs were then binned using MetaBAT v1.7. The quality (that is, completeness and contamination) of the reconstructed bingenomes was assessed using CheckM v1.0.18. Bingenomes with >85% completeness and <5% contamination were considered as successfully reconstructed and subject to downstream analysis. The taxonomic assignment of the reconstructed bingenomes was assessed using GTDB-TK v1.3.0, and the genome annotation was generated using RASTtk v1.073. The relative abundance of each reconstructed bingenome was calculated by mapping the quality-filtered sequence reads against the reconstructed bingenome using Bowtie2 v2.3.2. The percentage of mapped reads out of the total reads was regarded as the relative abundance of the reconstructed bingenome.

CTFE4 defluorination by pure cultures

The two pure cultures, that is, *S. sphaeroides* and *D. aminophilus*, were obtained from DSMZ-German Collection of Microorganisms and Cell Cultures under the DSM numbers 2875 and 12254, respectively. Both cultures were maintained in the same basal medium as used for the anaerobic biotransformation by the sludge community, as described above, with the addition of 20 mM sodium lactate as the electron donor. For the sulfate-reducing *D. aminophilus*, sodium sulfate (2 mM) was also added. For the **CTFE4** defluorination test, each culture was inoculated (10%, v/v) into 50 ml of fresh medium containing the same growth substrates and 50 μM **CTFE4**. After ~40 days, cells were collected by centrifugation at 18,000*g* for 20 min at room temperature for DNA extraction to determine the cell density (Supplementary Methods). The supernatant was subjected to F^- and **CTFE4** analysis.

Data availability

The metagenomic sequencing dataset has been deposited in the Sequence Read Archive under accession number PRJNA838587. Source data are provided with this paper. The draft genomes of the two dominant bacterial species in the isolated defluorinating colonies have been deposited in GenBank under the accession numbers JAMHFZ000000000 and JAMHGA000000000. All other data supporting the findings in this study are available within the paper and its Supplementary Information. Source data are provided with this paper.

References

1. Dolbier, W. R. Fluorine chemistry at the millennium. *J. Fluor. Chem.* **126**, 157–163 (2005).
2. Lohmann, R. et al. Are fluoropolymers really of low concern for human and environmental health and separate from other PFAS. *Environ. Sci. Technol.* **54**, 12820–12828 (2020).
3. Evich, M. G. et al. Per- and polyfluoroalkyl substances in the environment. *Science* **375**, eabg9065 (2022).
4. Xiao, F. Emerging poly- and perfluoroalkyl substances in the aquatic environment: a review of current literature. *Water Res.* **124**, 482–495 (2017).
5. Kotthoff, M. & Bucking, M. Four chemical trends will shape the next decade's directions in perfluoroalkyl and polyfluoroalkyl substances research. *Front. Chem.* **6**, 103 (2018).
6. Dams, R. & Hintzer, K. in *Fluorinated Polymers: Applications* Vol. 2 1–31 (The Royal Society of Chemistry, 2017).
7. Vanbrocklin, C. Military applications of chlorotrifluoroethylene oligomer base nonflammable hydraulic fluid. *J. Fire Sci.* **11**, 232–241 (1993).
8. Gschweder, L., Mattie, D., Syder, C., Warer, W. & van Brocklin, C. Chlorotrifluoroethylene oligomer based nonflammable hydraulic fluid. 1 Fluid, additive, and elastomer development. *J. Synth. Lubr.* **9**, 187–203 (1992).
9. Ellis, D. A., Mabury, S. A., Martin, J. W. & Muir, D. C. Thermolysis of fluoropolymers as a potential source of halogenated organic acids in the environment. *Nature* **412**, 321–324 (2001).
10. Myers, A. L., Jobst, K. J., Mabury, S. A. & Reiner, E. J. Using mass defect plots as a discovery tool to identify novel fluoropolymer thermal decomposition products. *J. Mass Spectrom.* **49**, 291–296 (2014).
11. Dias, J. et al. Thermal degradation behavior of ionic liquid/fluorinated polymer composites: effect of polymer type and ionic liquid anion and cation. *Polymer* **229**, 123995 (2021).
12. DelRaso, N. J., Auten, K. L., Higman, H. C. & Leahy, H. F. Evidence of hepatic conversion of C_6 and C_8 chlorotrifluoroethylene (CTFE) oligomers to their corresponding CTFE acids. *Toxicol. Lett.* **59**, 41–49 (1991).
13. Brashear, W. T., Greene, R. J. & Mahle, D. A. Structural determination of the carboxylic acid metabolites of polychlorotrifluoroethylene. *Xenobiotica* **22**, 499–506 (1992).
14. Song, X., Vestergren, R., Shi, Y., Huang, J. & Cai, Y. Emissions, transport, and fate of emerging per- and polyfluoroalkyl substances from one of the major fluoropolymer manufacturing facilities in China. *Environ. Sci. Technol.* **52**, 9694–9703 (2018).
15. Fujiwara, M., Jodry, J. J. & Narizuka, S. Process for producing alkoxycarbonylfluoroalkanesulfonates. US patent US20080108846A1 (2008).
16. Yin, H., Anders, M. W. & Jones, J. P. Metabolism of 1,2-dichloro-1-fluoroethane and 1-fluoro-1,2,2-trichloroethane: electronic factors govern the regioselectivity of cytochrome P450-dependent oxidation. *Chem. Res. Toxicol.* **9**, 50–57 (1996).
17. Harris, J. W. & Anders, M. W. Metabolism of the hydrochlorofluorocarbon 1,2-dichloro-1,1-difluoroethane. *Chem. Res. Toxicol.* **4**, 180–186 (1991).
18. Liu, J. & Mejia Avendano, S. Microbial degradation of polyfluoroalkyl chemicals in the environment: a review. *Environ. Int.* **61**, 98–114 (2013).
19. Yu, Y. et al. Microbial cleavage of C–F bonds in two C_6 per- and polyfluorinated compounds via reductive defluorination. *Environ. Sci. Technol.* **54**, 14393–14402 (2020).
20. Yu, Y. et al. Microbial defluorination of unsaturated per- and polyfluorinated carboxylic acids under anaerobic and aerobic conditions: a structure specificity study. *Environ. Sci. Technol.* **56**, 4894–4904 (2022).
21. Wackett, L. P. Nothing lasts forever: understanding microbial biodegradation of polyfluorinated compounds and perfluorinated alkyl substances. *Microb. Biotechnol.* **15**, 773–792 (2021).
22. Adrian, L. & Löffler, F. E. *Organohalide-Respiring Bacteria* (Springer, 2016).
23. Zhang, B. et al. Novel and legacy poly- and perfluoroalkyl substances (PFASs) in indoor dust from urban, industrial, and e-waste dismantling areas: the emergence of PFAS alternatives in China. *Environ. Pollut.* **263**, 114461 (2020).
24. Liu, W. et al. Atmospheric chlorinated polyfluorinated ether sulfonate and ionic perfluoroalkyl acids in 2006 to 2014 in Dalian, China. *Environ. Toxicol. Chem.* **36**, 2581–2586 (2017).
25. Wang, Y. et al. Suspect and nontarget screening of per- and polyfluoroalkyl substances in wastewater from a fluorochemical manufacturing park. *Environ. Sci. Technol.* **52**, 11007–11016 (2018).
26. Liu, Y., Qian, M., Ma, X., Zhu, L. & Martin, J. W. Nontarget mass spectrometry reveals new perfluoroalkyl substances in fish from the Yangtze River and Tangxun Lake, China. *Environ. Sci. Technol.* **52**, 5830–5840 (2018).

27. Washington, J. W. et al. Nontargeted mass-spectral detection of chloroperfluoropolyether carboxylates in New Jersey soils. *Science* **368**, 1103–1107 (2020).
28. MacInnis, J. J., Lehnherr, I., Muir, D. C. G., Quinlan, R. & De Silva, A. O. Characterization of perfluoroalkyl substances in sediment cores from High and Low Arctic lakes in Canada. *Sci. Total Environ.* **666**, 414–422 (2019).
29. Lin, Y., Ruan, T., Liu, A. & Jiang, G. Identification of novel hydrogen-substituted polyfluoroalkyl ether sulfonates in environmental matrices near metal-plating facilities. *Environ. Sci. Technol.* **51**, 11588–11596 (2017).
30. Yi, S., Zhu, L. & Mabury, S. A. First report on in vivo pharmacokinetics and biotransformation of chlorinated polyfluoroalkyl ether sulfonates in rainbow trout. *Environ. Sci. Technol.* **54**, 345–354 (2020).
31. Yi, S., Yang, D., Zhu, L. & Mabury, S. A. Significant reductive transformation of 6:2 chlorinated polyfluorooctane ether sulfonate to form hydrogen-substituted polyfluorooctane ether sulfonate and their toxicokinetics in male Sprague–Dawley rats. *Environ. Sci. Technol.* **56**, 6123–6132 (2021).
32. Lieberman, I. & Barker, H. A. β-Keto acid formation and decomposition by preparations of *Clostridium kluyveri*. *J. Bacteriol.* **68**, 329–333 (1954).
33. Buschmann, J., Angst, W. & Schwarzenbach, R. P. Iron porphyrin and cysteine mediated reduction of ten polyhalogenated methanes in homogeneous aqueous solution: product analyses and mechanistic considerations. *Environ. Sci. Technol.* **33**, 1015–1020 (1999).
34. Che, S. et al. Structure-specific aerobic defluorination of short-chain fluorinated carboxylic acids by activated sludge communities. *Environ. Sci. Technol. Lett.* **8**, 668–674 (2021).
35. Chen, G. et al. Anaerobic microbial metabolism of dichloroacetate. *mBio* https://doi.org/10.1128/mBio.00537-21 (2021).
36. Möller, B., Oßmer, R., Howard, B. H., Gottschalk, G. & Hippe, H. *Sporomusa*, a new genus of gram-negative anaerobic bacteria including *Sporomusa sphaeroides* spec. nov. and *Sporomusa ovata* spec. nov. *Arch. Microbiol.* **139**, 388–396 (1984).
37. Temme, H. R., Carlson, A. & Novak, P. J. Presence, diversity, and enrichment of respiratory reductive dehalogenase and non-respiratory hydrolytic and oxidative dehalogenase genes in terrestrial environments. *Front. Microbiol.* **10**, 1258 (2019).
38. Duhamel, M. & Edwards, E. A. Microbial composition of chlorinated ethene-degrading cultures dominated by *Dehalococcoides*. *FEMS Microbiol. Ecol.* **58**, 538–549 (2006).
39. Baena, S. et al. *Desulfovibrio aminophilus* sp. nov., a novel amino acid degrading and sulfate reducing bacterium from an anaerobic dairy wastewater lagoon. *Syst. Appl. Microbiol.* **21**, 498–504 (1998).
40. Yang, Y., Pesaro, M., Sigler, W. & Zeyer, J. Identification of microorganisms involved in reductive dehalogenation of chlorinated ethenes in an anaerobic microbial community. *Water Res.* **39**, 3954–3966 (2005).
41. *Water Quality—Determination of the Inhibitory Effect of Water Samples on the Light Emission of Vibrio fischeri (Luminescent Bacteria Test)—Part 3: Method Using Freeze-Dried Bacteria* ISO 11348-3:2007 (ISO, 2007).
42. Newton, S. et al. Novel polyfluorinated compounds identified using high resolution mass spectrometry downstream of manufacturing facilities near Decatur, Alabama. *Environ. Sci. Technol.* **51**, 1544–1552 (2017).
43. Evich, M. G. et al. Environmental fate of Cl-PFPECAs: predicting the formation of PFAS transformation products in New Jersey soils. *Environ. Sci. Technol.* **56**, 7779–7788 (2022).
44. Men, Y. et al. Sustainable syntrophic growth of *Dehalococcoides ethenogenes* strain 195 with *Desulfovibrio vulgaris* Hildenborough and *Methanobacterium congolense*: global transcriptomic and proteomic analyses. *ISME J.* **6**, 410–421 (2012).
45. Schymanski, E. L. et al. Identifying small molecules via high resolution mass spectrometry: communicating confidence. *Environ. Sci. Technol.* **48**, 2097–2098 (2014).
46. Tonomura, K., Futai, F., Tanabe, O. & Yamakoka, T. Defluorination of monofluoroacetate by bacteria. Part I. Isolation of bacteria and their activity of defluorination. *Agric. Biol. Chem.* **29**, 124–128 (1965).
47. Davis, C. K., Webb, R. I., Sly, L. I., Denman, S. E. & McSweeney, C. S. Isolation and survey of novel fluoroacetate-degrading bacteria belonging to the phylum *Synergistetes*. *FEMS Microbiol. Ecol.* **80**, 671–684 (2012).

Acknowledgements

This work was supported by the Strategic Environmental Research and Development Program (project no. ER20-1541, for B.J., Y.Y., J.G., J.L. and Y.M.) and the National Institute of Environmental Health Sciences (award no. R01ES032668, for H.L., S.C. and Y.M.). M. Elsner at the Technical University of Munich provided insightful discussion on the biodefluorination pathways.

Author contributions

Y.M. and B.J. conceived and designed the project, analysed the data and prepared the paper. B.J. conducted the anaerobic biotransformation experiments using the anaerobic microbial community and pure cultures and analysed the LC–HRMS/MS and sequencing data. S.C. performed the aerobic biotransformation experiments and contributed to the anaerobic biotransformation set-up. H.L. performed the anaerobic isolation and sample preparation for metagenomic sequencing. Y.Y. contributed to the analysis of the analytical and sequencing data. J.G. contributed to the calculation of the BDEs. J.L. contributed to the PFAS compound selection and mechanistic discussion.

Competing interests

The authors declare no competing interests.

Additional information

Supplementary information The online version contains supplementary material available at https://doi.org/10.1038/s44221-023-00077-6.

Correspondence and requests for materials should be addressed to Yujie Men.

Peer review information *Nature Water* thanks the anonymous reviewers for their contribution to the peer review of this work.